

On the validity of the method of reduction of dimensionality: area of contact, average interfacial separation and contact stiffness

I. A. Lyashenko,^{1,2} Lars Pastewka,^{3,4} and Bo N. J. Persson¹

¹*Peter Grünberg Institut-1, FZ-Jülich, 52425 Jülich, Germany*

²*Sumy State University, Rimskii-Korsakov Str. 2, 40007 Sumy, Ukraine*

³*Dept. of Physics and Astronomy, Johns Hopkins University, Baltimore, MD 21218, USA*

⁴*MikoTribologie Centrum μ TC, Fraunhofer-Institut für Werkstoffmechanik IWM, Freiburg, 79108 Germany*

It has recently been suggested that many contact mechanics problems between solids can be accurately studied by mapping the problem on an effective one dimensional (1D) elastic foundation model. Using this 1D mapping we calculate the contact area and the average interfacial separation between elastic solids with nominally flat but randomly rough surfaces. We show, by comparison to exact numerical results, that the 1D mapping method fails even qualitatively. We also calculate the normal interfacial stiffness K and compare it with the result of an analytic study. We attribute the failure of the elastic foundation model to the incorrect treatment of the long-range elastic coupling between the asperity contact regions.

1 Introduction

The calculation of the stress and displacement field resulting from the contact between elastic solids with rough surfaces is a very complex problem, in part due to the many length scales usually involved, and also because of the long-range elastic coupling between the contact regions. For this reason simplifying approaches are very important. However, most analytical theories, such as the Greenwood-Williamson (GW) contact mechanics theory [1], and the theory of Bush et al. [2], or theories based on the elastic foundation model (see Fig. 1), neglect the elastic coupling between asperity contact regions. It has recently been shown by exact numerical studies that the neglect of the elastic coupling results in qualitatively wrong contact topography [4], and even the relation between the contact force and the area of contact is incorrectly described using this approach [5]. In Ref. [6–8] it was also shown that the contact stress-stress correlation function scales as $q^{-\alpha}$ as a function of wavevector q , where in the overlap model $\alpha = 2 + H$ (where H is the Hurst exponent [9]), while including the long-range elastic coupling $\alpha = 1 + H$.

In a series of papers, Popov and coworkers have proposed that a simple 1D-elastic foundation model can be used to accurately describe the contact between elastic solids [10–13]. In a recent publication they calculated the normal stiffness between elastic solids with randomly rough but nominally flat surfaces, and argued that the

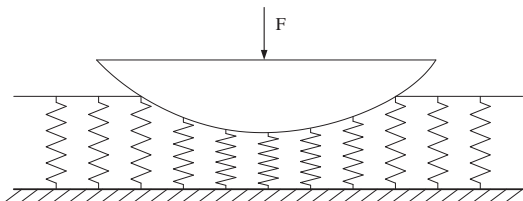


FIG. 1: In the elastic foundation model the elastic solid is replaced by an array of independent springs, see e.g., Ref. [3].

results are in good agreement with exact numerical results [13, 14]. In this note we will show that in fact this model fails even qualitatively to describe the contact mechanics correctly.

2 Method of reduction of dimensionality

For a semi-infinite elastic solid the surface displacement $u_z(\mathbf{x})$ can be directly related to the surface stress distribution $\sigma_z(\mathbf{x})$. This relation is particularly simple in wavevector space where

$$u_z(\mathbf{q}) = -(2/E^*q)\sigma_z(\mathbf{q}) \quad (1)$$

with contact modulus E^* . The contact modulus depends on Young's modulus E and Poisson's ratio ν , $E^* = E/(1 - \nu^2)$. From Eq. (1), it follows immediately that if a rigid axisymmetric object is squeezed against the elastic half space the surface stress and displacement fields will be related by a 1D-equation which depends only on the radial distance r from the center of the contact region. The general solution to this problem was obtained by Sneddon [15], who derived a 1D-integral equation from which the surface stress $\sigma_z(r)$ and surface displacement $u_z(r)$ can be derived for any shape of the axisymmetric punch, assuming the contact region is compact.

Geike, Heß and Popov [10, 11] have shown that the contact between a rigid axisymmetric indenter (punch), and an elastic half-space can be mapped on a 1D-problem where a 1D rigid contour is indented in a 1D-array of independent springs (1D-elastic foundation, see Fig. 1). The shape of the 1D contour can be determined from the shape of the original indenter using the equations derived by Sneddon [15]. The rule for mapping the axisymmetric 2D problem to 1D is

$$z_{1D}(x) = x \int_0^x dr \frac{\partial z / \partial r}{\sqrt{x^2 - r^2}}, \quad (2)$$

where $z(r)$ is the indenter shape. This mapping is only

part of Sneddon's solution for the total force F on an axisymmetric indenter. It lacks the factor of contact modulus E^* required to obtain a stress and an integral over x , $F = 2E^* \int_0^c dx (z_{1D}(c) - z_{1D}(x))$ where c is the contact radius. If the integral is discretized on a finite set of points spaced by a , then

$$F \approx \sum_{j=-c/a}^{c/a} aE^*(z_{1D}(c) - z_{1D}(ja)). \quad (3)$$

Eq. (3) suggests that F can be imagined as being given by compressing a series of (independent) springs with spring constant $k = aE^*$ with the profile $z_{1D}(x)$. Hence, a connection to Winkler's elastic foundation model can be drawn. This reformulation of Sneddon's equations has been dubbed the method of reduction of dimensionality (MRD). Note that the equations of Sneddon are only valid if the contact region is compact, and the 1D-mapping therefore also only holds as long as the contact region is compact [16]. In this limit, MRD gives the correct total force F on the indenter as a function of its displacement d . Note that for axisymmetric power-law indenters Eq. (2) maps onto a 1D profile with the same power [11]. For $z(r) = r^2$ one finds $z_{1D}(x) = 2x^2$.

The method of reduction of dimensionality has been applied to various problems with axisymmetry, but so far only to problems already solved by other methods. In addition, it is not clear to the present authors if there is any gain in computational effort in using the 1D-mapping approach, as compared to using the original 1D-equations derived by Sneddon, which was used to prove the MRD [10].

The invocation of the elastic foundation picture tempts to interpret the 1D elastic foundation literally. However, it has to be noted that for example the force on each spring *does not* represent the true pressure profile for the 3D contact problem. Also, the 1D rigid contour is not simply a slice through the 2D indenting surface, but rather given by the mapping Eq. (2). It is not clear what the mapping Eq. (2) would be for systems like, for example, the contact of two rigidly connected spheres. Some mapping could probably be found that correctly reproduces $F(d)$ obtained from a full 3D calculation. The important question is rather whether a *universal* mapping exists that does not necessitate the solution of the 3D problem and therefore saves computational effort. Such a universal mapping has been proposed for self-affine randomly rough surfaces [10], and later corrected to depend on Hurst-exponent H [14] (hence restricting universality to the class of self-affine surfaces with identical H). Here we show that this mapping fails even qualitatively for the randomly-rough surfaces considered here and can therefore not be universal.

3 Review of area of real contact and average interfacial separation for contacting rough surfaces

Consider two elastic solids with rough but nominally flat surfaces of nominal area A_0 , squeezed together by the nominal pressure $p = F/A_0$. We define the average interfacial separation as $\bar{u} = z_1 - z_0$, where z_1 is the the average position of the bottom surface of the upper solid and z_0 the average position of the upper surface of the bottom solid. As p increases, the average interfacial separation \bar{u} monotonically decreases, while the area of real contact A increases [17–20]. In earlier publications [18, 21–24] it has been shown that in a large pressure range $A \propto p$ and $\bar{u} \propto \ln p$. This can be understood as follows: As the load increases, existing contact patches grow and new, small contacts are formed. This happens in such a way that the distribution of contact sizes and local pressures remains approximately constant over a wide range of loads [18, 22]. It follows that $A \propto p$ and that the elastic deformation energy (per unit nominal contact area), U_{el} , stored at the interface must be proportional to the load or the nominal contact pressure [21]:

$$U_{el} = u_0 p, \quad (4)$$

where u_0 is a length parameter of order the root-mean-square (rms) roughness h_{rms} . Since the elastic energy is equal to the work done by the external load (assuming hard-wall interactions and no adhesion), it follows that

$$p = -\frac{dU_{el}}{d\bar{u}}.$$

Combining this with Eq. (1) gives

$$p = p_0 \exp(-\bar{u}/u_0), \quad (5)$$

where p_0 is an integration constant. The theory of Persson predicts that $u_0 = \alpha h_{rms}$ and $p_0 = \beta E^*$, where E^* is the effective elastic modulus and α (of order unity) and β are dimensionless. Both α and β only depend on the spectral properties of the surface [4, 21, 23–26].

In the same pressure range where (5) is valid, the area of real contact

$$\frac{A}{A_0} = \frac{\kappa p}{\xi E^*}, \quad (6)$$

where $\xi = \langle (\nabla h)^2 \rangle^{1/2}$ is the surface rms-slope and $\kappa \approx 2$.

Eqs. (5) and (6) are only valid at such high pressures that multi-asperity contact occurs. At very low pressures the solids will only make contact in the vicinity of the highest asperity. In this finite-size pressure region the relation between \bar{u} and p will exhibit large fluctuations from one surface realization to another [27]. In the study presented below the finite-size region is too small to be observed on the linear pressure scale used in Fig. 4. In Ref. [28] we have studied numerically and analytically the relation between the interfacial stiffness and the squeezing pressure in both the finite size pressure region and for higher pressures, and in Sec. 6 we compare these results

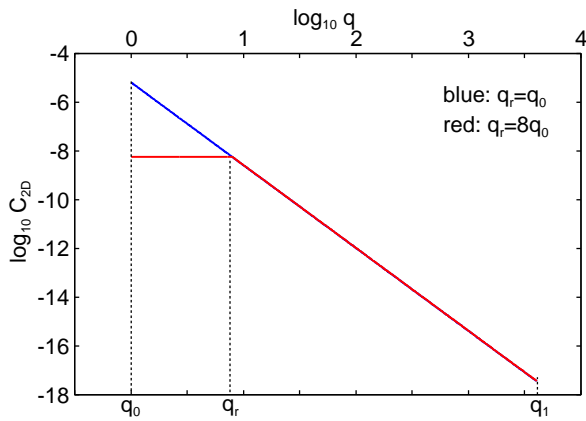


FIG. 2: The surface roughness power spectrum as a function of the wavevector (log-log scale) for a self-affine fractal surface with a roll-off (red line) and without roll-off (blue line). The two power spectrum's correspond to surfaces with the same root-mean-square (rms) slope 0.1 and Hurst exponent $H = 0.7$. The rms slope is determined mainly by the large wave vector region at $q \sim q_1$, and this is the reason for why the curves nearly overlap for $q > q_r$.

for the stiffness with the 1D-elastic foundation model of Popov et al.

4 Numerical test of reduction of dimensionality results for $A(p)$ and $u(p)$

In the MRD a 3D-contact problem is mapped on a 1D-elastic foundation problem. Here we are interested in the contact between two nominally flat but randomly rough surfaces. For frictionless contact, this problem can be mapped on an elastic half-space with a randomly rough surface in contact with a rigid substrate with a flat surface.

In the contact mechanics theory of Popov et al. the roughness of the 1D-substrate has a power spectrum related to that of the original via the equation:

$$C_{1D}(q) = \pi q C_{2D}(q). \quad (7)$$

The rationale behind C_{1D} is to produce a 1D-line profile that has the same mean-square (ms) roughness and ms curvature as the original 2D surface (with power spectrum C_{2D}). The ms slope of the 1D-line profile is half that of the 2D surface. Geike et al. [10] have shown that if the ms curvature is invariant, then the ms curvature of the asperity summits is about twice as large for the 1D profile as compared to the 2D profile. Therefore, the force-distance relationship for each individual asperity is maintained by the mapping Eq. (7) at small surface penetration (see section 2). Geike et al. [10] have also shown that the height distribution of asperities remains approximately invariant. Clearly, the model does not include elastic interactions between individual asperities and is therefore similar to GW or “bearing-area” theories [6]. Another source of error is that at large penetration of

the individual asperity into the bearing area the mapping Eq. (7) is not exact.

More recent formulations use a prefactor that depends on Hurst exponent H [14]. This modification does not affect the general conclusions drawn here. The spring constant of the elastic foundation is related to the effective (or combined) elastic modulus via $k = aE^*$, where a is the spacing between the springs (see Eq. (3)).

Using standard procedures we have generated randomly rough 1D-surfaces with the power spectra given by Eq. (7). As in an earlier study [28], the original 2D surface is self affine fractal with the Hurst exponent $H = 0.7$ (or fractal dimension $D_f = 3 - H = 2.3$) and with small and large cut-off wavevectors $q_0 = 2\pi/\sqrt{A_0}$ and $q_1/q_0 = 4096$. We consider two cases, namely when the substrate surface is fractal-like in the whole interval $q_0 < q < q_1$, and when there is a roll-off at $q_r/q_0 = 8$, see Fig. 2. The curves in Fig. 2 are the actual power spectrums we used in the calculations. Both curves correspond to surfaces with the same rms slope (equal to 0.1). The slope is determined mainly by the large wave vector region at $q \sim q_1$ and this is the reason for why the curves nearly overlap for $q > q_r$.

The red and blue solid lines in Fig. 3 have been calculated following the procedure outlined by Popov et al. [29–32]: Each independent spring is compressed into compliance by the 1D rough surface profile where the profile overlaps with the initial relaxed spring positions. In each step we calculated the force F and area of contact A . The applied force F was calculated as the sum of forces for all springs in contact:

$$F = k \sum_{i=1}^n \Delta u_i, \quad (8)$$

where n is the number of springs in contact, Δu_i is the spring compression. After this we have calculated the area of contact A [30–32]:

$$A = \frac{\pi}{4} \sum_{i=1}^{n_c} (an_i)^2, \quad (9)$$

where n_c is the number of connected regions. In this case all springs in connected regions must be in contact, n_i is the number of springs in each region, an_i are the diameters of these regions. Using Eq. (9) presumably implicitly assumes that the contact regions for the full 3D model are circular while in reality the contact regions have fractal-like boundaries. In the case of full contact $A = A_0$, where

$$A_0 = \frac{\pi}{4} (aN)^2, \quad (10)$$

and N is the full number of springs. Then there is only a single connected region, the diameter of which is equal to the length of the system aN . Using (8) and (10) we

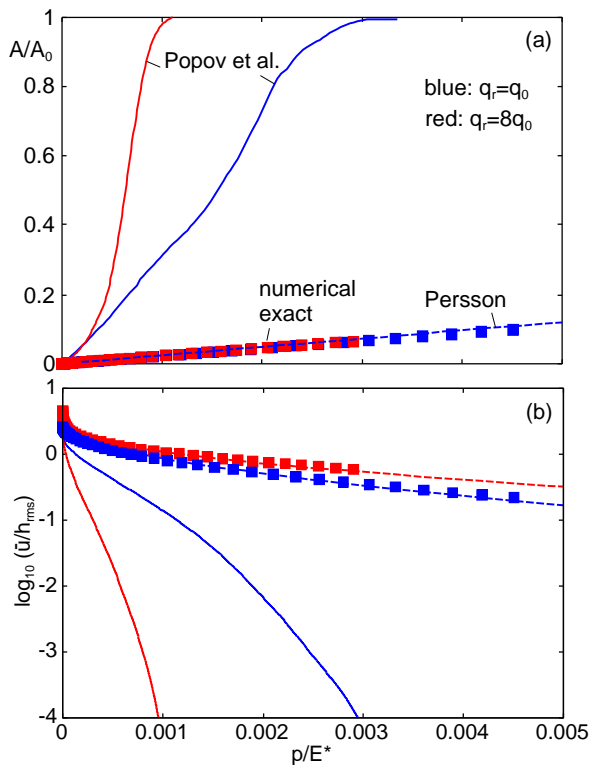


FIG. 3: (Color online) (a) The area of real contact A in units of the nominal contact area A_0 , and (b) the average interfacial separation \bar{u} in units of the rms roughness h_{rms} , as a function of the squeezing pressure p in units of the effective elastic modulus E^* . For self-affine fractal surfaces with $H = 0.7$ and rms-slope 0.1. The surfaces have the small and large wavevector cut-off $q_0 = 1$ and $q_1 = 4096$, respectively, and the roll-off wavevector $q_r = 1$ (blue curves) and $q_r = 8$ (red curves).

can also calculate the squeezing pressure $p = F/A_0$. The interfacial separation \bar{u} was calculated using the formula:

$$\bar{u} = \frac{1}{N} \sum_{i=1}^N u_i, \quad (11)$$

where u_i is the distance between the end of each spring and the substrate surface. For springs in contact $u_i = 0$.

Using this simple procedure we have calculated the MRD results for $A(p)$ and $u(p)$ as shown by the solid lines in Fig. 3a and 3b, respectively. The pressure was varied from zero up to full contact where $A(p) = A_0$. The results are obtained by averaging the calculated quantities over 100 realizations of the rough-line topography, with the 1D-power spectrum given by Eq. (7). In each realization the elastic foundation has 8192 springs.

We compare the predictions of the theory of Popov et al. with numerical exact results for the full 3D-problem (with 2D surfaces), obtained as described in Ref. [33, 34]. In brief, this method computes the surface displacements using a fast Fourier-transform technique with the linear surface Green's function given by Eq. (1) for Poisson ratio $\nu = 1/2$. The interaction with the rigid surface is treated

as a hard-wall repulsion. The solution for the contact geometry is found using a constrained conjugate-gradient algorithm until penetration into the rigid wall drops below a small tolerance ϵ . All area that feels a repulsive pressure is counted towards the contact area [35].

5 Numerical results for $A(p)$ and $\bar{u}(p)$

In Fig. 3(a) we show the calculated normalized contact area A/A_0 as a function of the squeezing pressure. The red and blue squares are the result of a numerically exact study and the dashed line the prediction using the theory of Persson. Since the two surfaces have the same rms slope the theory predicts the same curve for both cases, which agrees with the numerically exact results. The red and blue solid lines are the predictions using Popov's method. Since $A(p)$ approaches A_0 much faster in the MRD than in the numerically exact theory, the interfacial stiffness $K = -dp/d\bar{u}$ will approach infinity much faster (with increasing pressure) in the MRS, as compared to our exact numerical study. Thus the stiffness relation $K(p)$ will also be incorrectly given by the theory of Popov et al. (see also Sec. 6).

Fig. 3(b) shows the logarithm of the average interfacial separation \bar{u} as a function of the squeezing pressure p . Again there is good agreement between the numerically exact results and the theory of Persson, while the MRD fails qualitatively.

6 Contact stiffness

The total stiffness K_{tot} of the contact between two solids consists of a bulk part K_b related to compression of the solids and another part K from the approach of the two surfaces at the nominal contact area, which depends on the surface roughness of the two solids. For friction-less contact between two rectangular blocks $1/K_{tot} = 1/K_b + 1/K$. Here we will focus on the contribution K to the total contact stiffness. We can write $K = -dp/d\bar{u}$ where \bar{u} is the average interfacial surface separation (see Sec. 3).

Consider two elastic solids with nominally flat surfaces squeezed together by the nominal pressure $p = F/A_0$. From (5) it follows that the contact stiffness

$$K = -\frac{dp}{d\bar{u}} = \frac{p}{\alpha h_{rms}}$$

or

$$\frac{K h_{rms}}{E^*} = \frac{1}{\alpha} \frac{p}{E^*} \quad (12)$$

This equation is only valid at such high pressures that multi-asperity contact occurs. At very low pressures the solids will only make contact in the vicinity of the highest asperity. In this finite-size pressure region the relation between K and p will exhibit large fluctuations from one surface realization to another [27].

In Ref. [28] two of us have derived an (approximate) analytic expression for the (ensemble averaged) interfacial

stiffness in the finite-size region. The derivation assumes a self-affine fractal surface with the surface roughness power spectrum shown in Fig. 2. The surface is characterized by the Hurst exponent H and the small and large wavevector cut-off q_0 and q_1 , as well as a roll-off q_r (see Fig. 2). For this model the stiffness per unit area in the low pressure, finite size, region is approximately given by (see Ref. [28])

$$K \approx \left(\frac{E^*}{L^2 q_r} \right)^{H/(1+H)} \left(\frac{p}{h_{\text{rms}}} \right)^{1/(1+H)} \propto p^{1/(1+H)}$$

where $L \approx 2\pi/q_0$ is the linear size of the studied system. Note that we can also write this equation as

$$\frac{K h_{\text{rms}}}{E^*} \approx \left(\frac{h_{\text{rms}}}{L^2 q_r} \right)^{H/(1+H)} \left(\frac{p}{E^*} \right)^{1/(1+H)} \quad (13)$$

The same scaling has been obtained in Ref. [13] from scaling arguments. These scaling arguments do however not give a fully parameter free expression for K that includes all prefactors.

7 Numerical results for $K(p)$

We consider again two cases, when the substrate surface is fractal-like in the whole interval $q_0 < q < q_1$, and when there is a roll-off at $q_r = 8$ (see Fig. 2). In Fig. 4(a) we show the calculated interfacial stiffness using the theory of Persson. We have plotted $K h_{\text{rms}}/E^*$ as a function of p/E^* since these are the dimensionless quantities that enter in the theory [see Eqs. (12) and (13)]. The results in Fig. 4(a) are in excellent agreement with exact numerical simulations for the same system (see Fig. 1 in Ref. [28]). One can distinguish three regions in the stiffness $K(p)$ relation. For very small pressures the stiffness increases as $K \propto p^{1/(1+H)}$. This is a finite size effect, which occurs when a single effective Hertzian contact region, formed at the highest substrate asperity, prevails. For higher pressures a region where $K \propto p$ is observed. This region, which becomes wider as the width of the roll-off region increases, results from contact with many asperities, and depends crucially on the long-range elastic coupling between the contact regions. Finally, for very large pressure the interfacial separation approaches zero and the interfacial stiffness increases towards infinite.

Fig. 4(b) shows the results using the contact mechanics theory of Popov et al. The results are again obtained by averaging the contact stiffness obtained in 100 realizations of the rough-line topography, with the 1D-power spectrum given by Eq. (7). In each realization the elastic foundation has 8192 springs. Fig. 4(b) shows that the theory correctly predicts the initial (low pressure) relation $K \propto p^{1/(1+H)}$. This result is expected because the study in Ref. [28] shows that $K \propto p^{1/(1+H)}$ holds even when one neglects the elastic coupling between the asperity contact regions. However, the region where K increases linearly with the pressure p is absent in Fig.

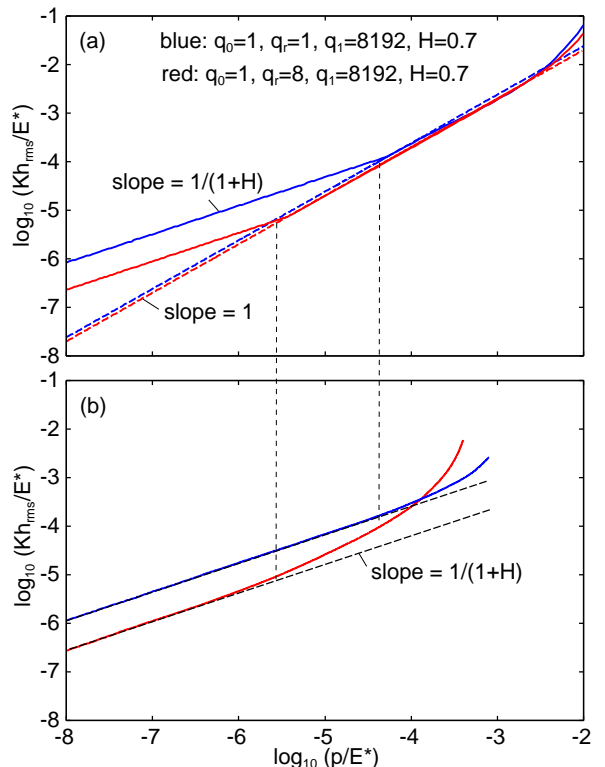


FIG. 4: (Color online) Log-log plot of the nondimensional contact stiffness $K h_{\text{rms}}/E^*$ vs. nondimensional pressure p/E^* for self-affine fractal surfaces with $H = 0.7$ and rms slope 0.1. The surfaces have the small and large wavevector cut-off $q_0 = 1$ and $q_1 = 4096$, respectively, and the roll-off wavevector $q_r = 1$ (blue curves) and $q_r = 8$ (red curves). The result in (a) is from the Persson contact mechanics theory, which agrees with the exact numerical study presented in Ref. [28]. The result in (b) is using the theory of Popov et al. The vertical dashed lines indicate the pressures where the Popov et al. theory starts to deviate from the analytic results.

4(b). This is also expected because the $K \propto p$ result depends crucially on the elastic coupling between the asperity contact regions, which is not included in the theory of Popov et al. As shown in Fig. 4(a), the linear region is particularly large when there is a roll-off in the power spectrum. Most surfaces of engineering interest exhibit a roll-off even larger than for the $q_r/q_0 = 8$ case shown in Fig. 2. Thus in most practical applications, in particular involving elastically soft materials like rubber, one will be in the linear $K \propto p$ region where the MRD fails.

We note that whether there is a roll-off or a cut-off at q_r has very little influence on the result. However, this does not imply that the only thing which matters is the range over which the surface is self-affine fractal. The point is that including a roll-off or cut-off at $q_r > q_0$ implies roughly that the surface is “periodically” repeated $(q_r/q_0)^2$ times. This implies that there will be many asperities of height similar to the highest asperity. This in turn means that the contact will much more quickly (with

increasing pressure) come into the multi-asperity contact configuration where the stiffness K depends linearly on the nominal squeezing pressure p . This is the origin of why the linear relation between K and p starts at lower pressures, and extends over a larger pressure range, when the surface has a roll-off or cut-off.

The vertical dashed lines in Fig. 4 indicate the pressures where the theory of Popov et al. starts to deviate from the analytic results in Fig. 4(a). Note that these points correspond to the start of the linear $K \propto p$ region in the analytic theory. This is expected as the linear region corresponds to multi-asperity contact, where the elastic coupling between the asperity contact regions, which is incorrectly treated in the Popov et al. theory, becomes important. Thus we believe it is the incorrect treatment of the long range elasticity, and not the reduction in dimensionality, which is the basic problem with the approach of Popov et al (see also Ref. [36]).

8 Summary and conclusion

We have presented a detailed comparison of the theory of Popov et al., dubbed the method of reduction of dimensionality (MRD), with numerical exact results and analytic results for self-affine fractal surfaces with and without a roll-off. The MRD fails qualitatively to describe the $A(p)$ and $\bar{u}(p)$ relations, and we attribute this to the incorrect treatment of the elastic coupling between the asperity contact regions. Indeed, Popov recently acknowledged that results obtained for the contact area can be wrong in some circumstances [14]. A recent study by Scaraggi et al.[36] has shown that if the long-range elastic coupling is properly included in the analysis, it is possible to make 2D isotropic roughness approximately equivalent to 1D roughness.

We have also presented a detailed comparison of the MRD with analytic results for the normal contact stiffness. For the case of a roll-off at $q_r = 8$ the Persson theory and the exact numerical results presented in Ref. [28], exhibit a linear $K \propto p$ region extending over 3 decades in pressure, while there is no linear region in the MRD. The latter theory predicts $K \propto p^{1/(1+H)}$ in the limit of small pressures, but this result is expected since an effective Hertz single-asperity contact prevails in this case (see Ref. [28]). However, since the elastic coupling between the asperity contact regions is incorrectly treated in the approach of Popov et al., no linear $K \propto p$ region is obtained.

Acknowledgments We thank Giuseppe Carbone, Martin Müser and Mark Robbins for useful discussions. L.P. acknowledges funding from the European Commission (Marie-Curie IOF-272619).

-
- [1] Greenwood, J.A., Williamson, J.B.P.: Contact of nominally flat surfaces. Proc R Soc A **295**, 300 (1966)
 - [2] A.W. Bush, R.D. Gibson and T.R. Thomas: The elastic contact of a rough surface. Wear **35**, 87 (1975).
 - [3] See, e.g., Sec. 4.3 in K.L. Johnson, *Contact Mechanics*, Cambridge University Press (1985).
 - [4] Almqvist, A., Campaña, C., Prodanov, N., Persson, B.N.J.: Interfacial separation between elastic solids with randomly rough surfaces: Comparison between theory and numerical techniques. J Mech Phys Solids **59** 2355 (2011)
 - [5] Carbone, G., Bottiglione, F.: Asperity contact theories: Do they predict linearity between contact area and load? J Mech Phys Solids **56**, 2555 (2008)
 - [6] Ramisetti, S.B., Campaña, C., Anciaux, G., Molinari, J.-F., Müser, M. H., Robbins, M.O.: The autocorrelation function for island areas on self-affine surfaces. J Phys Condens Matter **23**, 215004 (2011)
 - [7] Campaña, C, Müser, M.H., Robbins, M.O.: Elastic contact between self-affine surfaces: comparison of numerical stress and contact correlation functions with analytic predictions. J Phys Condens Matter **20**, 354013 (2008)
 - [8] Persson, B.N.J.: Capillary adhesion between elastic solids with randomly rough surfaces. J Phys Condens Matter **20**, 315007 (2008)
 - [9] Meakin, P.: *Fractals, scaling and growth far from equilibrium*, Cambridge University Press (1998)
 - [10] Geike, T., Popov, V.L.: Mapping of three-dimensional contact problems into one dimension. Phys Rev E **76**, 036710 (2007)
 - [11] Heß, M.: *Über die Abbildung ausgewählter dreidimensionaler Kontakte auf Systeme mit niedrigerer räumlicher Dimension*, Cuvillier-Verlag (Göttingen, 2011)
 - [12] Pohrt, R., Popov, V.L.: Normal contact stiffness of elastic solids with fractal rough surfaces. Phys Rev Lett **108**, 104301 (2012)
 - [13] Pohrt, R., Popov, V.L., Filippov, A.É.: Normal contact stiffness of elastic solids with fractal rough surfaces for one- and three-dimensional systems. Phys Rev E **86**, 026710 (2012)
 - [14] In a recent paper published after we had submitted this manuscript [V.L. Popov: Method of reduction of dimensionality in contact and friction mechanics: A link between micro and macro scales, Friction **1**, 41 (2013)] Popov states: “In Ref. [9] the size of the system was accidentally chosen in such a way that the area-force dependence was correct up to relative large contact. This result, however, cannot be generalized.”
 - [15] Sneddon, I.N.: The relation between load and penetration in the axisymmetric Boussinesq problem for a punch of arbitrary profile. Int J Eng Sci **3**, 47 (1965)
 - [16] Barber, J.R., private communication
 - [17] Persson, B.N.J.: Theory of rubber friction and contact mechanics. J Chem Phys **115**, 3840 (2001)
 - [18] Hyun, S., Pei, L., Molinari, J.-F., Robbins, M.O.: Finite-element analysis of contact between elastic self-affine surfaces. Phys Rev E **70**, 026117 (2004)
 - [19] Berthoud, P., Baumberger, T.: Shear stiffness of a solid-solid multicontact interface. Proc R Soc A **454**, 1615 (1998)
 - [20] Barber, J.R.: Bounds on the electrical resistance between

- contacting elastic rough bodies. *Proc R Soc A* **459**, 53 (2003)
- [21] Persson, B.N.J.: Relation between interfacial separation and load: A general theory of contact mechanics. *Phys Rev Lett* **99**, 125502 (2007)
- [22] Campañá, C., Müser, M.H.: Contact mechanics of real vs. randomly rough surfaces: A Green's function molecular dynamics study. *EPL* **77**, 38005 (2007)
- [23] Campañá, C., Persson, B.N.J., Müser, M.H.: Transverse and normal interfacial stiffness of solids with randomly rough surfaces. *J Phys Condens Matter* **23**, 085001 (2011)
- [24] Akarapu, S., Sharp, T., Robbins, M.O.: Stiffness of contacts between rough surfaces. *Phys Rev Lett* **106**, 204301 (2011)
- [25] Carbone, G., Scaraggi, M., Tartaglino, U.: Adhesive contact of rough surfaces: Comparison between numerical calculations and analytical theories. *Eur Phys J E* **30**, 65 (2009)
- [26] Carbone, G., Bottiglione, F.: Contact mechanics of rough surfaces: a comparison between theories. *Meccanica* **46**, 557 (2011)
- [27] Lorenz, B., Persson, B.N.J.: Interfacial separation between elastic solids with randomly rough surfaces: comparison of experiment with theory. *J Phys Condens Matter* **21**, 015003 (2009)
- [28] Pastewka, L., Prodanov, N., Lorenz, B., Müser, M.H., Robbins, M.O., Persson, B.N.J.: Finite-size scaling in the interfacial stiffness of rough elastic contacts. *Phys Rev E* **87**, 062809 (2013)
- [29] Popov, V.L., Filippov, A.É.: Force of friction between fractal rough surface and elastomer. *Technical Physics Letters* **36**, 525 (2010)
- [30] See Chapter 19 in: V.L. Popov, *Contact Mechanics and Friction, Physical Principles and Applications* Springer, Berlin (2010)
- [31] See articles in: *Physical Mesomechanics* **15**, No. 4 (2012).
- [32] Popov, V.L., Filippov, A.É.: Applicability of a reduced model to description of real contacts between rough surfaces with different Hirsch indices. *Technical Physics Letters* **34**, 722 (2008)
- [33] Campañá, C., Müser, M.H.: Practical Green's function approach to the simulation of elastic semi-infinite solids. *Phys Rev B* **74**, 075420 (2006)
- [34] Pastewka, L., Sharp, T.A., Robbins, M.O.: Seamless elastic boundaries for atomistic calculations. *Phys Rev B* **86**, 075459 (2012)
- [35] Polonsky, I.A., Keer, L.M.: A numerical method for solving rough contact problems based on the multi-level multi-summation and conjugate gradient techniques. *Wear* **231**, 206 (1999)
- [36] Scaraggi, M., Putignano, C., Carbone, G.: Elastic contact of rough surfaces: A simple criterion to make 2D isotropic roughness equivalent to 1D one. *Wear* **297** 811 (2013)